Impact of terrestrial biosphere carbon exchanges on the anomalous CO_2 increase in 2002–2003

W. Knorr,[1] N. Gobron,[2] M. Scholze,[1] T. Kaminski,[3] R. Schnur,[4] and B. Pinty[2]

Received 6 December 2006; revised 20 February 2007; accepted 3 April 2007; published 5 May 2007.

[1] Understanding the carbon dynamics of the terrestrial biosphere during climate fluctuations is a prerequisite for any reliable modeling of the climate-carbon cycle feedback. We drive a terrestrial vegetation model with observed climate data to show that most of the fluctuations in atmospheric CO_2 are consistent with the modeled shift in the balance between carbon uptake by terrestrial plants and carbon loss through soil and plant respiration. Simulated anomalies of the Fraction of Absorbed Photosynthetically Active Radiation (FAPAR) during the last two El Niño events also agree well with satellite observations. Our model results suggest that changes in net primary productivity (NPP) are mainly responsible for the observed anomalies in the atmospheric CO_2 growth rate. Changes in heterotrophic respiration (R_h) mostly happen in the same direction, but with smaller amplitude. We attribute the unusual acceleration of the atmospheric CO_2 growth rate during 2002–2003 to a coincidence of moderate El Niño conditions in the tropics with a strong NPP decrease at northern mid latitudes, only partially compensated by decreased R_h. **Citation:** Knorr, W., N. Gobron, M. Scholze, T. Kaminski, R. Schnur, and B. Pinty (2007), Impact of terrestrial biosphere carbon exchanges on the anomalous CO_2 increase in 2002–2003, *Geophys. Res. Lett.*, *34*, L09703, doi:10.1029/2006GL029019.

1. Introduction

[2] It is now widely accepted that increasing levels of CO_2 in the atmosphere can lead to a positive feedback effect of climate warming, because the warming itself may cause the terrestrial biosphere to emit additional CO_2 compared to no climate change [*Knorr et al.*, 2005a; *Friedlingstein et al.*, 2006]. However, the underlying mechanisms that govern the response of the terrestrial biosphere to climate changes and fluctuations are still a matter of debate. It is therefore of particular importance to investigate the causes of recent climate fluctuations and how they are linked to observed changes in the atmospheric CO_2 growth rate. Such anomalous increases happened during the extreme El Niño event of 1997/1998, and during 2002/2003.

[3] A link between the El Niño/Southern Oscillation (ENSO) phenomenon and the rate of atmospheric CO_2 increase has been established a while ago [*Keeling et al.*, 1989; *Rayner et al.*, 1999; *Bousquet et al.*, 2000; *C. D. Jones et al.*, 2001; *Zeng et al.*, 2005a], with CO_2 rising more rapidly during warm, so called El Niño phases. A more recent study also shows a consistent link between El Niño and drought in the tropics [*Lyon*, 2004]. It is of major interest to assess the likely mechanism behind recent interannual fluctuations of atmospheric CO_2, which can then be used to assess if similar mechanisms may indeed cause a positive feedback to climate warming.

[4] In this study, we first revisit the established link between atmospheric CO_2, ENSO, and global land precipitation. We then drive a terrestrial vegetation model with interannual climate observations to establish whether the processes implemented within this model can explain the observed interannual fluctuations in the atmospheric CO_2 growth rate. We use independent satellite data of observed vegetation activity to cross-check simulated vegetation response during September 1997–August 1998, as well as September 2002–August 2003, i.e. the last two pronounced El Niño episodes. Previous studies have suggested either that the European drought has contributed significantly to the anomalous CO_2 rise [*Ciais et al.*, 2005], that 2002/2003 was anomalous in the sense that the usual link between ENSO and CO_2 increases broke down and CO_2 increased more than expected [*Jones and Cox*, 2005], or that wide-spread drought conditions in the tropics [*Knorr et al.*, 2005b] or northern mid latitudes [*Zeng et al.*, 2005b] were the cause.

2. Data and Model Description

[5] To simulate both terrestrial-biosphere carbon fluxes and FAPAR, we use the terrestrial ecosystem model BETHY [*Knorr*, 2000] driven by daily values of minimum and maximum temperature, precipitation, and solar incoming radiation for the period 1 January 1979 to 30 June 2005. Output for the year 1979 is disregarded to avoid remaining effects of model spin-up in the soil moisture pools of BETHY. For comparing results obtained with BETHY directly with observations, we feed net CO_2 fluxes from BETHY into the TM2 transport model to simulate CO_2 mixing ratios at the same stations, Mauna Loa and South Pole [*Kaminski et al.*, 1999] and apply the same algorithm to compute low-pass filtered time derivatives as with the NOAA/CMD observations (see next).

[6] For the model, we use climate input data of land precipitation and daily minimum and maximum temperatures. Daily values of those variables and of solar incoming radiation are generated on a global 2° latitude by 2° longitude grid using the method of *Nijssen et al.* [2001], based on daily station data from the Summary of

[1] Quantifying and Understanding the Earth System Research (QUEST), Department of Earth Sciences, University of Bristol, Bristol, UK.
[2] Institute for Environment and Sustainability, European Commission Joint Research Centre, Ispra, Italy.
[3] FastOpt, Hamburg, Germany.
[4] Max-Planck-Institute for Meteorology, Hamburg, Germany.

0094-8276/07/2006GL029019$05.00

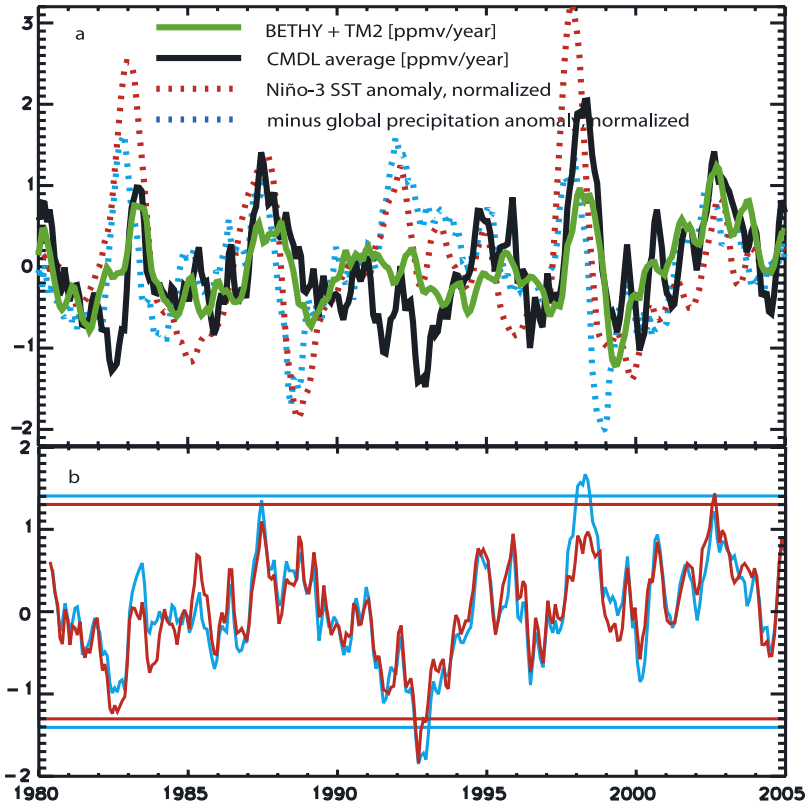

Figure 1. (a) Growth rate anomalies of atmospheric CO_2 derived from the average of the atmospheric mixing ratios at Mauna Loa, Hawaii, and the South Pole, in ppm year^{-1}, and anomalies of Niño-3 (5°N–5°S, 150°W–90°W) SSTs and global land precipitation times minus 1, normalized by their respective standard deviation (SSTs: 0.99°C, global average land precipitation: 0.98 mm/month); all periods with reference to Jan 1980 to Dec 2004. (b) Residuals of two linear statistical models of the CO_2 growth rate, using Niño-3 SSTs (red) or global land precipitation anomalies (blue) as a predictor. Horizontal lines denote 99% confidence levels of the respective model, assuming the residual is Gaussian distributed.

the Day Observations (Global CEAS), National Climatic Data Center, and monthly gridded data. Monthly gridded temperature are obtained from the most recent update of the data set of *P. D. Jones et al.* [1999, 2001], with gaps filled from data of *Hansen et al.* [1999, 2001]. Monthly gridded precipitation data come from a 1.0° version of *Chen et al.* [2002]. We document changes in vegetation activity using the monthly, gridded 0.5° by 0.5° FAPAR product of *Gobron et al.* [2005] from September 1997 to June 2005. From this time series, we subtract the average seasonal cycle, to obtain average anomalies for the two 12-month periods September 1997–August 1998 and September 2002–August 2003, discarding grid cells with monthly data gaps for these periods. For atmospheric CO_2, we use the average of the monthly data from the continuous and the flask sampling program of the National Oceanic and Atmospheric Administration's Climate Monitoring Division (CMD) [*Conway et al.*, 1994] from July 1979 to March 2005. We take the average of two stations, Mauna Loa and South Pole, to obtain an approximate global average and compute the monthly growth rate minus the average seasonal cycle during the years 1980 to 2004. This time series is then low-pass filtered by a 7-month running mean, a time-scale at which each hemisphere can be considered well-mixed [*Kaminski et al.*, 1999]. We use an efficient matrix representation of the atmospheric transport model TM2 [*Kaminski et al.*, 1999] to simulate the CO_2 mixing ratio at the same stations from the net CO_2 fluxes calculated by BETHY. We neglect ocean, land use and fossil fuel fluxes as they are believed to contribute less to interannual fluctuations [*Le Quéré et al.*, 2003; *Zeng et al.*, 2005a]. Finally, we use monthly Niño-3 sea surface temperatures (SST) from NOAA Climate Prediction Centre (available at http://www.cpc.noaa.gov/data/indices/) to document the state of ENSO.

3. Results

[7] The first analysis concerns only observations, and reveals a strong link between anomalous CO_2 rise in the atmosphere, global land precipitation anomalies, and ENSO (see Figure 1a). The CO_2 growth rate lags behind both global land precipitation and Niño-3 sea surface temperature anomalies (SSTs). Cold phases of ENSO, so-called La Niña events, appear to be linked to anomalously slow CO_2 increase. The only major deviation is found for 1991–1993 coinciding with the time after the eruption of Mount Pinatubo, which has lead to a wide-spread cooling, presumably offsetting the effects of a moderate El Niño event during that time [*Jones and Cox*, 2001, 2005].

[8] The fastest increase in CO_2 during this record (Figure 1a) was in early 1998 and coincided with the

strongest El Niño event, which started in late 1997. 2003 saw an almost equally fast CO_2 increase, while the El Niño event during this time was among the weakest since 1980. It is interesting to note that 2002 was almost as dry globally as 1997/1998, and dryer than 2003. Also, the period 2002/2003 appears unusual with global land precipitation very low for only a moderate El Niño event.

[9] To further examine the possible causes of the CO_2 fluctuations, we develop two linear statistical models similar to the one by *Jones and Cox* [2005]:

$$\frac{dc}{dt}(t) = a_1 + b_1 T(t - t_1) + d_1 N$$

$$\frac{dc}{dt}(t) = a_2 + b_2 P(t - t_2) + d_2 N$$

c is the atmospheric CO_2 mixing ratio in ppm, T the Niño3-SST anomaly in K, P the global land precipitation anomaly in mm/month, and N a Gaussian distributed random variable. The lag times, t_1 and t_2 (integer multiples of 1 month), and the constants a_i, b_i, and d_i are fitting parameters, where d_i is equal to the root-mean-squared error of the linear model. The best fit is achieved with t_1 = 4 months and t_2 = 5 months, $a_1 = -0.005$, $b_1 = 0.338$, $d_1 = 0.560$; $a_2 = -0.010$, $b_2 = -0.373$, $d_2 = 0.604$ (units in ppm/yr, except ppm/yr/K for b_1 and ppm/yr/(mm/month) for b_2). Excluding the Pinatubo period from this analysis had only a small effect on the analysis. The residuals of these models are displayed in Figure 1b. Horizontal lines indicate the respective 99% confidence intervals of random fluctuations. As shown earlier by *Jones and Cox* [2005], a linear model based on ENSO shows significant deviation from observations during the Pinatubo period 1991–1993, and for the more recent El Niño event of 2002/2003. Apart from the Pinatubo years, the model based on global land precipitation significantly deviates from observations during 1997/1998, but is consistent with the 2002/2003 anomaly. These results indicate that for 2002/2003, drought not related to El Niño played a more important role in creating the anomalous CO_2 increase compared to the El Niño event of 1997/1998, while the latter event seems more related to El Niño SSTs than to precipitation changes.

[10] An analysis using simulated CO_2 fluxes from the terrestrial biosphere model reveals that the processes of photosynthesis, plant and soil respiration that are represented within BETHY can explain most of the observed fluctuations in atmospheric CO_2 (see Figure 1a). Since the ocean reacts to ENSO out of phase compared to the land but with a smaller magnitude [*C. D. Jones et al.*, 2001; *Zeng et al.*, 2005a], we would expect a smaller amplitude of growth rate anomalies by up to 20% if ocean fluxes had been included into the simulations. Further examination of Figure 1a shows that the CO_2 growth rate anomalies simulated with BETHY are less than observed during the strong El Niño of 1997/1998, while for 2002/2003 both agree rather well. During the dry season in late 1997, large peatland fires were observed in Indonesia, emitting an estimated 0.8 to 2.6 PgC into the atmosphere [*Page et al.*, 2002], corresponding to 0.4 to 1.2 ppm, consistent with observations [*Rödenbeck et al.*, 2003]. Since fires are not included in BETHY, this might explain the difference between the simulated and observed CO_2 growth rate. We also examined the growth rate for Mauna Loa and South Pole separately (not shown), and find that for 2002/2003 it is 0.4 to 0.5 ppm/yr higher in the northern hemisphere (Mauna Loa), while the simulated difference is only 0.1 to 0.2 ppm/yr. Fires in Siberia during 2003 might have contributed an additional CO_2 source, but estimates of 0.08 PgC emitted tend to be low, although highly uncertain [*Balzter et al.*, 2005].

[11] As shown by *Knorr et al.* [2005b], the transition from the 1999/2000 La Niña event until about mid 2003 was accompanied by increasing global land dryness. The impact of this temporary drying trend were not only visible in satellite derived FAPAR, but it could also be well reproduced with BETHY. Here, we focus on a comparison of BETHY derived and satellite observed FAPAR anomalies between the 1997/1998 and the 2002/2003 event which were both characterized by particularly large positive anomalies of the atmospheric CO_2 growth rate. Both 1-year periods analyzed start in September and end in August. The observed FAPAR anomaly pattern shown in Figure 2a for 1997/1998 is typical of El Niño conditions, negative for Sumatra, Java, Australia, northern South America to Central America, and positive at the Peruvian coast, southern and Baja California, southern Brazil to Argentina, as well as southern Africa [*Ropelewski and Halpert*, 1987; *Larkin and Harrison*, 2005], if we expect vegetation to be primarily rainfall limited in those areas. For 2002/2003, the observed pattern is less typical of El Niño conditions (Figure 2c): notably, the Peruvian coast and the area around Baja California have lower than normal FAPAR, indicating dryer than normal conditions,, highly unusual for El Niño. In general, the extreme El Niño of 1997/1998 appears to have led to a net increase in vegetation activity, despite anomalously low precipitation (see Figure 1a), while 2002/2003 saw an almost universal decrease.

[12] BETHY reproduces the observed patterns of FAPAR change generally well (see Figures 2b and 2d), especially in the tropics. Southern South America, western North America, East Africa, India, eastern Australia and the Mediterranean Basin show positive, central South America, Central America, southern, central and West Africa, and Southeast Asia negative FAPAR anomalies for 1997/1998. For 2002/2003, simulations show more widespread negative anomalies, especially in Southern Africa, Australia, India, Europe and North America. The areas with the largest negative anomalies observed are shown in Table 1. Note that both Europe and Australia have comparable magnitudes, which exceed one standard deviation of interannual variability (which is 0.016 for both). But since the area affected is much larger, Australia contributes a much greater proportion to the global area-integrated negative anomaly in 2002/2003. India and southern Africa also contribute somewhat more than Europe.

[13] An important question to be addressed is how these FAPAR anomalies translate into anomalies in the net ecosystem exchange (NEE), which is defined as R_h–NPP, i.e. as a net flux into the atmosphere. We would expect to see an analogous decrease in NPP with a decrease in FAPAR, but it is less clear how R_h would change. BETHY simulations for the 2002/2003 anomaly generally show the expected pattern of NPP change (Table 1), but the corre-

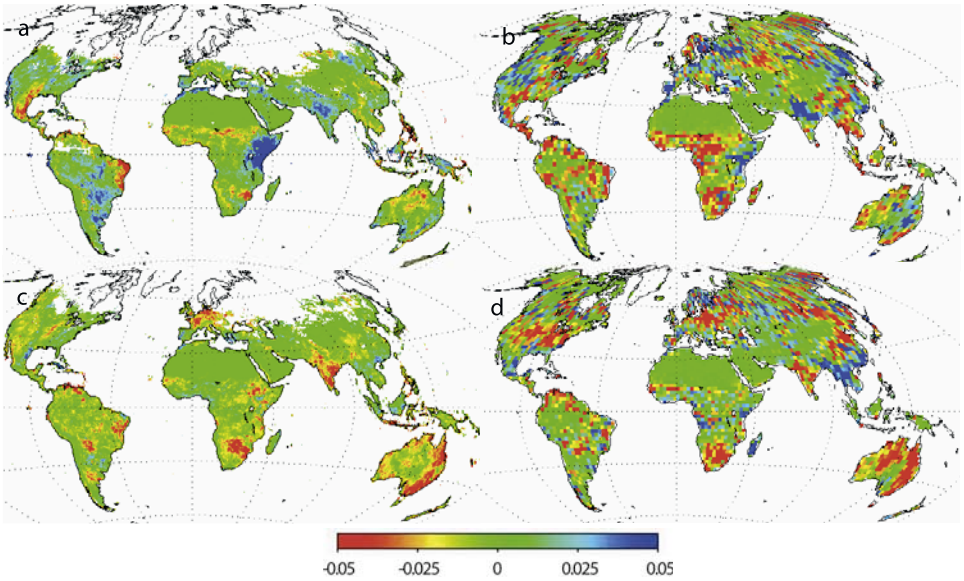

Figure 2. (a) Anomalies of FAPAR for September 1997 to August 1998 retrieved from SeaWiFS satellite data. Only data points where all 12 months were present are shown. Anomalies were obtained by subtracting the average seasonal cycle during September 1997 to June 2005. (b) The same FAPAR simulated by the BETHY model. (c) Anomalies of FAPAR for September 2002 to August 2003 retrieved from SeaWiFS satellite data. (d) The same simulated with BETHY.

spondence is not linear. Area-weighted, simulated FAPAR change, expressed as % of global total, can be directly related to the area-integrated NPP change (in PgC), and this shows an over-proportional NPP decrease for Europe (−0.024PgC per % of global FAPAR anomaly) compared to the other areas (all ca. −0.012PgC per %). R_h also responds to the climate anomaly by a decrease, which partially compensates the NPP. Here, Australia is the region where the R_h response is largest, and Europe where it is smallest. As a consequence, both regions contribute similar magnitudes to the simulated NEE anomaly, even though FAPAR and NPP are effected much more. We have to note, however, that this analysis relies on the simulated fluxes, and that BETHY underestimates the FAPAR anomaly in Europe, but overestimates the Australian one.

[14] An important finding, however, is that NPP changes in general tend to be accompanied by R_h changes in the same direction, counteracting part of the impact on CO_2 fluxes, and this deserves further examination at the global scale. Figure 3b shows that in the tropics, all El Niño events show this general pattern, which is opposite to the findings presented by *Zeng et al.* [2005a], who state that opposite changes in NPP and R_h through ENSO cycles add up to create the observed CO_2 growth anomalies. For the global anomalies (Figure 3a), two events stand out showing an exceptionally large negative NPP anomaly: 1982/1983 and 2002/2003, but interestingly not 1997/1998, even though it had the highest positive NEE anomaly. We find the following explanation: 1982/1983 is fully dominated by tropical fluxes, but 1997/1998 coincides with a positive NPP and R_h anomaly at northern mid latitudes, leading to an overall R_h increase globally and less NPP decrease than expected. This, however, has no impact on NEE. For 2002/2003, moderate anomalies in the tropics as expected by the strength of the ENSO signal coincide with a large and prolonged NPP anomaly at northern mid latitudes extending from mid 1999 until then end of 2003, only partially compensated by R_h decreases. Both act together to create a relatively large positive anomaly of the atmospheric CO_2 growth rate. The results partially agree with the finding of *Zeng et al.* [2005b], who simulated a similar, but larger NEE anomaly in the same latitude band, shifted one year forward (1998–2002). The timing we find, however, agrees better with atmospheric inversions results [*Rödenbeck et al.*, 2003; *Zeng et al.*, 2005b], which show an anomalous source at high latitudes starting in 2000.

4. Conclusions

[15] This analysis has shown that model results representing changes in the balance between plant uptake of CO_2 by terrestrial plants and CO_2 release by soils are consistent with

Table 1. Area Averaged Anomalies of FAPAR From SeaWiFS Satellite Data and FAPAR (Unitless), and Area Integrated Anomalies of NPP, R_h and NEE From BETHY Simulations for Key Regions During September 2002 to August 2003 for Areas With a Complete 12-Month Record[a]

	Central Europe	India	South Africa	Australia
ΔFAPAR SeaWiFS	−0.023 (7.0%)	−0.020 (9.6%)	−0.020 (10.7%)	−0.021 (25.1%)
ΔFAPAR BETHY	−0.017 (8.0%)	−0.016 (8.4%)	−0.026 (18.9%)	−0.031 (40.4%)
ΔNPP	−0.19	−0.10	−0.22	−0.49
ΔR_h	−0.05	−0.05	−0.08	−0.31
ΔNEE	0.14 (9.5%)	0.05 (3.4%)	0.13 (9.1%)	0.18 (12.2%)

[a]BETHY simulations, in PgC. Key regions: Central Europe, 10°W–30°E, 45°N–55°N; India, 70°E–90°E, 5°N–30°N; South Africa, 15°E–35°E, 35°S–15°S; Australia, 110°E–155°E, 45°S–10°S. Reference period is September 1997 to June 2005. Percentage figures in parentheses indicate the fraction of the global anomaly, defined as the area-integrated anomaly of the region divided by the area-integrated global anomaly.

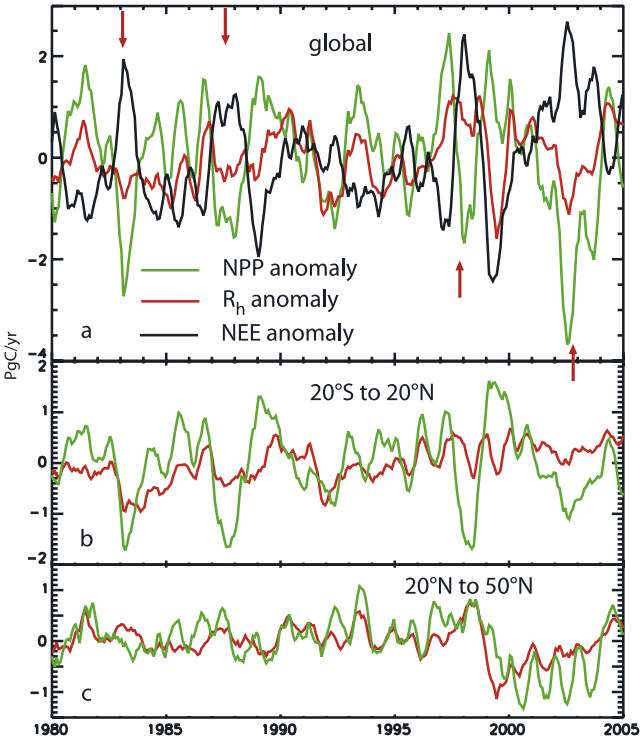

Figure 3. Anomalies of NPP, R_h, and NEE simulated with BETHY globally and for selected latitude bands, shown as 7-month running means: (a) global, (b) tropics (20°S to 20°N) and (c) northern mid-latitudes (20°N to 50°N). Reference period is January 1980 to December 2004. Red arrows mark major El Niño events.

the observed fluctuation in the atmospheric CO_2 growth rate at the interannual time scale. A test of model results against both atmospheric CO_2 measurements and satellite observed vegetation activity shows good agreement, further supporting this hypothesis. For particular instances, such as the 1997/1998 extreme El Niño event, the assumption of additional CO_2 sources, such as from fires, is necessary to explain the observations. For the anomalous CO_2 rise during 2002–2003, we find that it was probably caused by extremely widespread drought conditions in 2002 and 2003. A significant part of the anomaly was contributed by northern mid latitudes, whereas the response of the terrestrial biosphere in the tropics was rather typical of a moderate El Niño event. Other anomalous CO_2 sources in the northern hemisphere may have also contributed, e.g. fires in Siberia [*Balzter et al.*, 2005]. Our simulations show that Europe contributed about 10% to the NEE anomaly for September 2002 to August 2003, or about 0.14 PgC. Since European FAPAR anomalies are underestimated by about a quarter, we might expect a larger value if the model was adjusted to match the observed FAPAR, even though less than the 0.5 PgC estimated by *Ciais et al.* [2005]. In general, we find that the remarkable feature of the 2002–2003 anomaly seems to be that climate fluctuations, not only related to El Niño and occurring across all latitudes, acted together to create an unusually strong outgasing of CO_2 of the terrestrial biosphere. Further research will be required to investigate if this fluctuation carries features of projected future climate change and the CO_2 growth rate anomaly has been a first indicator of a developing positive feedback between climate warming and the global carbon cycle.

[16] **Acknowledgments.** We thank two anonymous reviewers for their helpful comments on the manuscript, and T. J. Conway and the Global Monitoring Division/Earth Systems Research Laboratory of NOAA for provision of the data of CO_2 atmospheric mixing ratios. This work was support by the QUEST program of the Natural Environment Research Council, U.K.

References

Balzter, H., et al. (2005), Impact of the Arctic Oscillation pattern on interannual forest fire variability in Central Siberia, *Geophys. Res. Lett.*, *32*, L14709, doi:10.1029/2005GL022526.

Bousquet, P., P. Peylin, P. Ciais, C. Le Quere, P. Friedlingstein, and P. P. Tans (2000), Regional changes in carbon dioxide fluxes of land and oceans since 1980, *Science*, *290*, 1342–1346.

Chen, M., P. Xie, J. E. Janowiak, and P. A. Arkin (2002), Global Land Precipitation: A 50-yr monthly analysis based on gauge observations, *J. Hydrometeorol.*, *3*, 249–266.

Ciais, P., et al. (2005), Europe-wide reduction in primary productivity caused by the heat and drought in 2003, *Nature*, *437*, 529–533.

Conway, T. J., P. P. Tans, L. S. Waterman, K. W. Thoning, D. R. Kitzis, K. A. Mararie, and N. Zhang (1994), Evidence for interannual variability of the carbon cycle from the NOAA/CMDL global air sampling network, *J. Geophys. Res.*, *99*, 22,831–22,855.

Friedlingstein, P., et al. (2006), Climate-carbon cycle feedback analysis, results from the C4MIP model intercomparison, *J. Clim.*, *19*, 3337–3353.

Gobron, N., B. Pinty, F. Mélin, M. Taberner, M. M. Verstraete, A. Belward, T. Lavergne, and J.-L. Widlowski (2005), The state of vegetation in Europe following the 2003 drought, *Int. J. Remote Sens.*, *26*, 2013–2020.

Hansen, J., R. Ruedy, J. Glascoe, and M. Sato (1999), GISS analysis of surface temperature change, *J. Geophys. Res.*, *104*, 30,997–31,022.

Hansen, J., R. Ruedy, M. Sato, M. Imhoff, W. Lawrence, D. Easterling, T. Peterson, and T. Karl (2001), A closer look at United States and global surface temperature change, *J. Geophys. Res.*, *106*, 23,947–23,963.

Jones, C. D., and P. M. Cox (2001), Modeling the volcanic signal in the atmospheric CO_2 record, *Global Biogeochem. Cycles*, *15*, 453–465.

Jones, C. D., and P. M. Cox (2005), On the significance of atmospheric CO_2 growth rate anomalies in 2002–2003, *Geophys. Res. Lett.*, *32*, L14816, doi:10.1029/2005GL023027.

Jones, C. D., M. Collins, P. M. Cox, and S. A. Spall (2001), The carbon cycle response to ENSO: A coupled climate-carbon cycle model study, *J. Clim.*, *14*, 4113–4129.

Jones, P. D., M. New, D. E. Parker, S. Martin, and I. G. Rigor (1999), Surface air temperature and its variations over the last 150 years, *Rev. Geophys.*, *37*, 173–199.

Jones, P. D., T. J. Osborn, K. R. Briffa, C. K. Folland, B. Horton, L. V. Alexander, D. E. Parker, and N. A. Rayner (2001), Adjusting for sampling density in grid-box land and ocean surface temperature time series, *J. Geophys. Res.*, *106*, 3371–3380.

Kaminski, T., M. Heimann, and R. Giering (1999), A coarse grid three-dimensional global inverse model ot the atmospheric transport: 1. Adjoint model and Jacobian matrix, *J. Geophys. Res.*, *104*, 18,535–18,553.

Keeling, C. D., R. B. Bacastow, A. F. Carter, S. C. Piper, T. P. Whorf, M. Heimann, W. G. Mook, and H. Roeloffzen (1989), A three-dimensional model of atmospheric CO_2 transport based on observed winds: 1. Analysis of observational data, in *Aspects of Climate Variability in the Pacific and Western Americas*, *Geophys. Monogr. Ser.*, vol. 55, edited by D. H. Peterson, pp. 277–303, AGU, Washington D. C.

Knorr, W. (2000), Annual and interannual CO_2 exchanges of the terrestrial biosphere: Process-based simulations and uncertainties, *Global Ecol. Biogeogr.*, *9*, 225–252.

Knorr, W., I. C. Prentice, J. I. House, and E. A. Holland (2005a), Long-term sensitivity of soil carbon turnover to warming, *Nature*, *433*, 298–301.

Knorr, W., M. Scholze, N. Gobron, B. Pinty, and T. Kaminski (2005b), Global-Scale Drought Caused Atmospheric CO_2 Increase, *Eos Trans. AGU*, *86*(18), 178–181.

Larkin, N. K., and D. E. Harrison (2005), Global seasonal temperature and precipitation anomalies during El Niño autumn and winter, *Geophys. Res. Lett.*, *32*, L16705, doi:10.1029/2005GL022860.

Le Quéré, C., et al. (2003), Two decades of ocean CO_2 sink and variability, *Tellus, Ser. B*, *55*, 649–656.

Lyon, B. (2004), The strength of El Niño and the spatial extent of tropical drought, *Geophys. Res. Lett.*, *31*, L21204, doi:10.1029/2004GL020901.

Nijssen, B., R. Schnur, and D. P. Lettenmaier (2001), Global retrospective estimation of soil moisture using the VIC land surface model, 1980–1993, *J. Clim.*, *14*, 1790–1808.

Page, S. E., F. Siegert, J. O. Rieley, H.-D. V. Boehm, A. Jayak, and S. Limink (2002), The amount of carbon released from peat and forest fires in Indonesia during 1997, *Nature*, *420*, 61–65.

Rayner, P. J., R. M. Law, and R. Dargaville (1999), The relationship between tropical CO_2 fluxes and the El Nino-Southern Oscillation, *Geophys. Res. Lett.*, *26*, 493–496.

Rödenbeck, C., S. Houweling, M. Gloor, and M. Heimann (2003), CO_2 flux history 1982–2001 inferred from atmospheric data using a global inversion of atmospheric transport, *Atmos. Chem. Phys. Disc.*, *3*, 2575–2659.

Ropelewski, C. F., and M. S. Halpert (1987), Global and regional scale precipitation patterns associated with the El Niño/Southern Oscillation, *Mon. Weather Rev.*, *115*(8), 1606–1626.

Zeng, N., A. Mariotti, and P. Wetzel (2005a), Terrestrial mechanisms of interannual CO_2 variability, *Global Biogeochem. Cycles*, *19*, GB1016, doi:10.1029/2004GB002273.

Zeng, N., H. Qian, C. Rödenbeck, and M. Heimann (2005b), Impact of 1998–2002 midlatitude drought and warming on terrestrial ecosystem and the global carbon cycle, *Geophys. Res. Lett.*, *32*, L22709, doi:10.1029/2005GL024607.

N. Gobron and B. Pinty, Institute for Environment and Sustainability, EC Joint Research Centre, T.P. 440, Via E. Fermi, I-21020 Ispra, Italy.

T. Kaminski, FastOpt, Schanzenstraβe 36, D-20357 Hamburg, Germany.

W. Knorr and M. Scholze, QUEST, Department of Earth Sciences, University of Bristol, Bristol BS8 1RJ, UK. (wolfgang.knorr@bristol.ac.uk)

R. Schnur, Max-Planck-Institute for Meteorology, Bundesstr. 53, D-20146 Hamburg, Germany.